The dynamic response of the Cable-suspended Parallel Robot hanged on the four points and powered by four motors

Mirjana Filipovic
Mihajlo Pupin Institute, University of Belgrade, Belgrade, Serbia
e-mail: mira @robot.imp.bg.ac.rs
mirjana.filipovic@pupin.rs

Abstract— **The Cable-suspended Parallel Robot hanged on four points powered by four motors (CPR) is very attractive and interesting to engineering and scientific community due to its future intensive development. The aim of the research in this paper is to define the dynamic model of CCPR system hanged on four points which will follow and record a moving object with high precision wherever the object moves in the workspace. Each contribution is a step closer to the realization of highly automated systems which would precisely lead camera in the area with as less involvement of human interference as possible. Such CPR functionality can only be provided by formulating and applying its highly authentic mathematical model during synthesis and analysis which will enable further development and implementation of the current control laws.**

Keywords-observation; workspace; geometry; forces; dynamic; analysis.

I. INTRODUCTION

A well-defined mathematical model of CPR is a step closer to the realization of highly automated CPR, which will lead a camera precisely in the area with as less human participation as possible. Similar systems have been analyzed and modeled which has been presented through numerous publications.

In paper [1], the design of a planar three-degree-of-freedom parallel manipulator is considered from a kinematic viewpoint. Four different design criteria are established and used to produce designs having optimum characteristics.

The paper [2] presents the first and second order kinematic analysis of a three-degree-of- freedom 3-RPS parallel robot mechanism. The position and orientation parameters of the moving platform of this mechanism are six.

In paper [3] authors present algorithms that enable precise trajectory control of NIMS3D, an under constrained, three-dimensional cabled robot intended for use in actuated sensing. They begin by offering a brief system overview and then describe methods to determine the range of operation of the robot. Next, a discrete-time model of the system is resented.

In paper [4] author presents several prototypes of wire-driven parallel robots, recently designed and which use two different actuation schemes. Two of them have been completed and submitted to extensive tests. These tests have allowed determining interesting open problems related to kinematics that are presented.

The wrench-closure workspace of parallel cable-driven mechanisms is the set poses of their mobile platform for which the cables can balance any external wrench. The determination of this workspace is an important issue in [5] since the cables can only pull and not push on the mobile platform.

Parallel cable-driven Stewart-Gough platforms consist of an end-effector which is connected to the machine frame by motor driven cables. Since cables can transmit only tension forces, at least m = n + 1 cables are needed to tense a system having n degrees-of-freedom. This results in a kinematical redundancy and leads to a (m – n)-dimensional solution space for the cable force distribution presented in [6].

This paper presents the recent results from a newly designed parallel wire robot which is currently under construction. Firstly, an overview of the system architecture is given and technically relevant requirements for the realization are identified. A technique to compute and transfer an estimation of the workspace to CAD tools is presented in [7].

The paper [8] presents an auto-calibration method for over constrained cable-driven parallel robots using internal position sensors located in the motors. A calibration workflow is proposed and implemented including pose selection, measurement, and parameter adjustment.

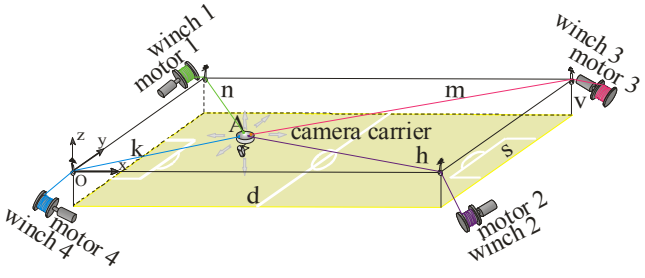

Figure 1. CCPR, in the space.

Wire-driven parallel robot has attracted the interest of researchers since the very beginning of the study of parallel robots [9]. This type of robot has the advantage of having light mobile mass, simple linear actuators with possibly relatively large stroke and less risk of interference between the legs. On the other hand their major drawback is that wire actuator can only pull and not push.

This work was done for the suspension system in four points, i.e. to be hung on all four edges of the workspace shape parallelepiped. It is a necessary geometric condition so as to provide camera motion through the entire space. See Fig. 1 and 2.

The CPR system has different areas of applications and promising research future. Our goal is to implement this system with maximum precision.

The Section II represents a detailed description of the dynamic model for the CCPR system. The sample of the system response is analyzed in section III. In the section IV there are concluding remarks.

II. Dynamic Model of CPR System

In this paper a special case of the constructive CPR model solution, has been analyzed. This model is named CCPR, and it is presented in Figs. 1. The property of the CCPR system is that each direction has one rope.

The novelty of this research is a methodology for generating a dynamic model of the CCPR system.

A CCPR operates by using four ropes that are fixed in maximum four corners of the observed space. See Figs.1 and 2.

By rotating the angular positions of each motor θ_1, θ_2, θ_3, θ_4, the winches of radius R rotate directly, which will wind or unwind ropes synchronously and it will accordingly move camera carrier in the Cartesian space x, y, z.

The desired trajectory of motion of the camera is defined in the Cartesian space x, y, z, and implemented by angular positions of each motor θ_1, θ_2, θ_3, θ_4.

This relationship is defined by the Jacobian matrix J_∇, which connects velocities of external coordinates $\dot{p} = [\dot{x} \quad \dot{y} \quad \dot{z}]^T$ and velocities of internal coordinates $\dot{\phi} = [\dot{\theta}_1 \quad \dot{\theta}_2 \quad \dot{\theta}_3 \quad \dot{\theta}_4]^T$.

For any trajectory generation in x, y, z space, it is necessary to provide very precise and mutually coordinated motion for all four motors θ_1, θ_2, θ_3, θ_4.For making of the CCPR system, it was necessary first to define the Jacobian matrix J_∇, as a connection of the velocities of the external coordinates changes $\dot{p} = [\dot{x} \quad \dot{y} \quad \dot{z}]^T$ and velocities of the internal coordinates changes $\dot{\phi} = [\dot{\theta}_1 \quad \dot{\theta}_2 \quad \dot{\theta}_3 \quad \dot{\theta}_4]^T$.

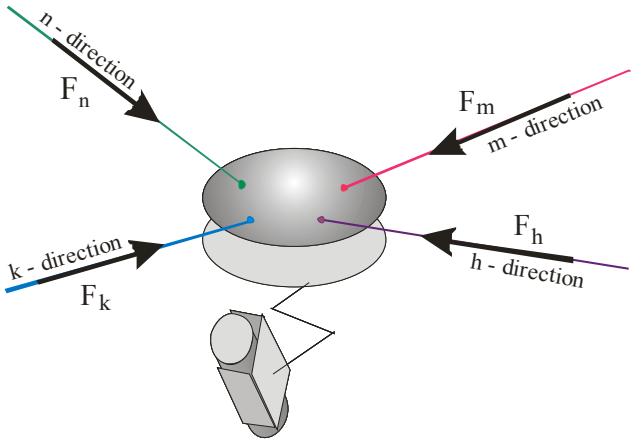

Figure 2. The ropes forces which carry a camera.

The forces in the ropes which carry a camera are shown in Fig. 2.

$$\dot{\phi} = J_\nabla \cdot \dot{p}. \tag{1}$$

$$J_\nabla = \begin{bmatrix} J_{\nabla 11} & J_{\nabla 12} & J_{\nabla 13} \\ J_{\nabla 21} & J_{\nabla 22} & J_{\nabla 23} \\ J_{\nabla 31} & J_{\nabla 32} & J_{\nabla 33} \\ J_{\nabla 41} & J_{\nabla 42} & J_{\nabla 43} \end{bmatrix}. \tag{2}$$

Equation (2) defined only for CCPR. If the camera motion is defined in x, y, z space, equation (2) is required in order to define the motion of all four motors. The mathematical model of the CCPR system has the following form:

$$u = G_v \cdot \ddot{\phi} + L_v \cdot \dot{\phi} + S_v \cdot M_\nabla. \tag{3}$$

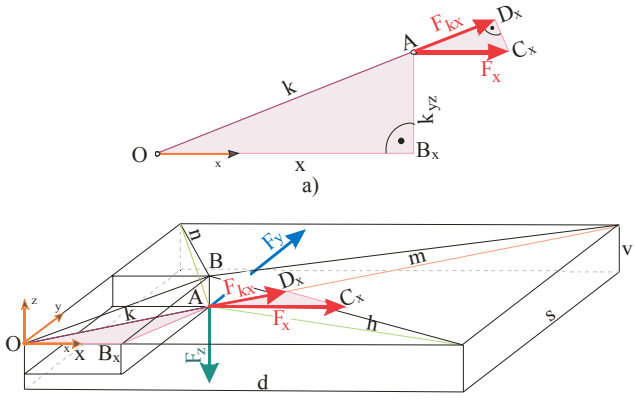

Figure 3. A characteristic triangle in the x - k plane.

Vector equation (3) is based on the Lagrange's equation of motion using the generalized coordinates θ_1, θ_2, θ_3, θ_4. The motors load is defined with the vector's equation (21). The motors load is defined with the vector's equation (21).

$$M_\nabla = F_\nabla \cdot R. \tag{4}$$

The force $F_\nabla = [F_1 \quad F_2 \quad F_3 \quad F_4]^T$ is acting on the shaft of each motor, and its value depends on the external forces F.

$$F = F_p + P_p. \tag{5}$$

$$F_p = m \cdot (\ddot{p} + a_{cc}). \tag{6}$$

In the Fig. 3a, two similar right-angled triangles can be seen. These triangles are in the x - k plane, which is clearly depictured in Fig. 3b. The hypotenuse of the OAB_x triangle has the length k, which is changeable during the camera motion. The other two sides of the OAB_x triangle have sizes x and $K_{yz} = \sqrt{y^2 + z^2}$. The component of the external force F in the x direction is F_x and the projection of the force F_x on the k direction is F_{kx} which can be seen in Fig. 3. The similarities of the two triangles in Fig. 3 produce the following relations:

$$\frac{x}{k} = \frac{F_{kx}}{F_x}. \tag{7}$$

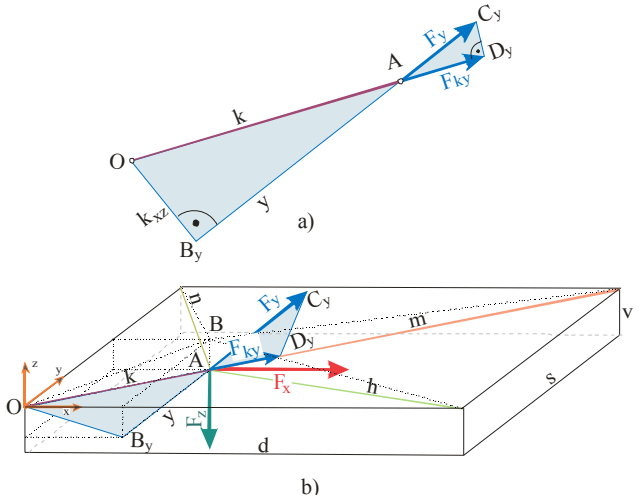

b)

Figure 4. A characteristic triangle in the y - k plane.

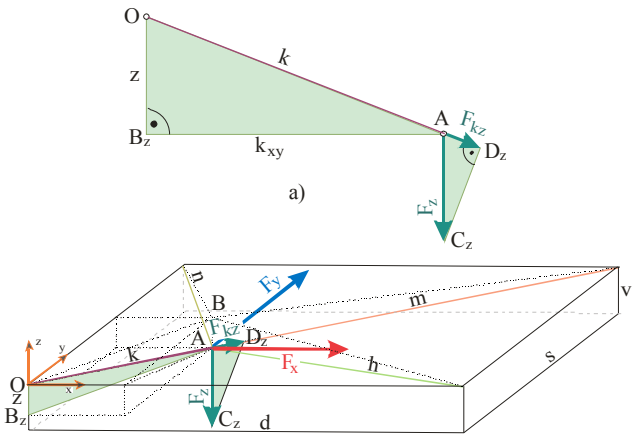

b)

Figure 5. A characteristic triangle in the z - k plane.

$$F_{kx} = \frac{x}{k} \cdot F_x. \tag{8}$$

In the Fig. 4a, another two similar right-angled triangles are shown.

These triangles are placed in the y - k plane.

The two sides of the OAB_y triangle have sizes y and $K_{xz} = \sqrt{x^2 + z^2}$. The component of the external force F in the y direction is F_y and the projection of the force F_y on the k direction is F_{ky} which can be seen in Fig. 4. The similarities of the two triangles in Fig. 4 produce the following relations:

$$\frac{y}{k} = \frac{F_{ky}}{F_y}. \tag{9}$$

$$F_{ky} = \frac{y}{k} \cdot F_y. \tag{10}$$

In the Fig. 5, two more similar right-angled triangles are shown. These triangles are in the z - k plane.

The hypotenuse of the OAB_z triangle has the length k.

The other two sides of the OAB_z triangle have sizes z and $k_{xy} = \sqrt{x^2 + y^2}$.

The component of the external force F in the z direction is F_z and the projection of the force F_z on the k direction is F_{kz} which can be seen in Fig. 5. The similarities of the two triangles in Fig. 5 produce the following relations:

$$\frac{z}{k} = \frac{F_{kz}}{F_z}. \tag{11}$$

$$F_{kz} = \frac{z}{k} \cdot F_z. \tag{12}$$

The force F_k is a sum of the previously defined components in (8), (10), (12), and it is expressed in the following equation:

$$F_k = F_{kx} + F_{ky} + F_{kz} = \frac{x}{k} \cdot F_x + \frac{y}{k} \cdot F_y + \frac{z}{k} \cdot F_z. \tag{13}$$

By using geometric properties of the similar triangles, and the methodology from the previous procedure, we have defined the forces F_h, F_m, F_n, in the other three ropes.

$$F_h = F_{hx} + F_{hy} + F_{hz}. \tag{14}$$

$$F_m = F_{mx} + F_{my} + F_{mz}. \tag{15}$$

$$F_n = F_{nx} + F_{ny} + F_{nz}. \tag{16}$$

The native of the mechanism construction creates dependency of the forces F_k, F_h, F_m and F_n, and the forces F_1, F_2, F_3, F_4:

$$F_1 = F_n, \quad F_2 = F_h, \quad F_3 = F_m, \quad F_4 = F_k. \tag{17}$$

See Fig. 1 and 2.

The forces F_1, F_2, F_3, or F_4 are generated and they produce the load on the shaft of the related motors through the radius R of the corresponding winder.

Following this procedure, the relationship between the resultant forces and the total external force can be defined in a vector form. See equation (18).

$$\begin{bmatrix} F_1 \\ F_2 \\ F_3 \\ F_4 \end{bmatrix} = \begin{bmatrix} C_{\nabla 11} & C_{\nabla 12} & C_{\nabla 13} \\ C_{\nabla 21} & C_{\nabla 22} & C_{\nabla 23} \\ C_{\nabla 31} & C_{\nabla 32} & C_{\nabla 33} \\ C_{\nabla 41} & C_{\nabla 42} & C_{\nabla 43} \end{bmatrix} \cdot \begin{bmatrix} F_x \\ F_y \\ F_y \end{bmatrix}. \tag{18}$$

By substituting equations (4) and (18) into the equation (3), the dynamic model of CCPR has been generated:

$$u = G_v \cdot \ddot{\phi} + L_v \cdot \dot{\phi} + S_v \cdot R \cdot C_{\nabla} \cdot F. \tag{19}$$

The matrix C_{∇} indicates that the system is highly coupled.

The developed dynamic model shows that there is the influence of the mechanism dynamic parameters onto the camera carrier dynamics.

The motor selection significantly affects the dynamics of the system.

Control law is selected by the local feedback loop for the position and velocity of the motor shaft in the following form:

$$u_i = K_{lpi} \cdot (\theta_i^o - \theta_i) + K_{lvi} \cdot (\dot{\theta}_i^o - \dot{\theta}_i). \tag{20}$$

The CPR device is developed in the Mihajlo Pupin Institute and is used to observe space. It is a part of more complex system presented in [10]. Simulation Results

III. PROGRAM PACKAGE ARRO

The CCPR system is modeled and analyzed by the software package ARRO. The software package ARRO is used for validation of applied theoretical contributions.

It is important to notice that the software package ARRO contains few essential subroutines, for example subroutine for kinematics of CCPR system, subroutine for dynamic of CCPR system and subroutine in which control law for the motion of CCPR is developed. Mathematical model of the motor is an integral part of software package ARRO. Through the simulation results it is shown that the dynamic characteristics of the motor significantly affect the response of the system and its stability. Kinematics and dynamics of the mechanism, dynamics of the motor and selected control structure are not independent entities but interwoven structures and that reflects in complexity of the observed system CCPR.

The CCPR model has been analyzed using the defined trajectory and system parameters. The camera moves in 3D space (x, y and z directions).

The camera carrier position has starting point $p^o_{start} = [1.8 \quad 0.3 \quad -0.3](m)$, and the end point $p^o_{end} = [1.2 \quad 0.9 \quad -0.9](m)$.

The shape of the velocity graph is trapezoidal with the maximum velocity $\dot{p}^o_{\max} = 0.417[m/s]$.

The motors are Heinzman SL100F type and gears are HFUC14-50-2A-GR+belt type.

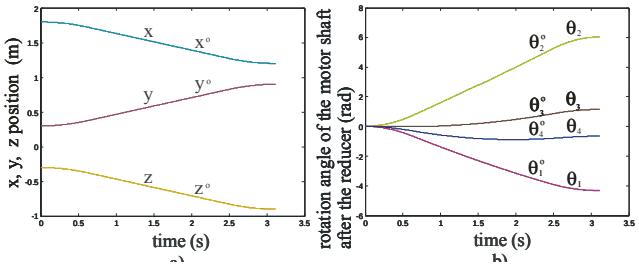

Figure 6. Reference frame and real frame a) x , y , z of camera carrier, b) θ_1 , θ_2 , θ_3 , θ_4 of motor shaft.

The mathematical model of the system, at the reference frame is defined by (1)-(19).

A camera carrier is under the influence of the disturbance force $F_p = \left[(200 \cdot \sin(4 \cdot \pi \cdot t) + 100 \cdot \sin(8 \cdot \pi \cdot t)) \quad 0 \quad 0\right]^T$, which simulates the impact of the wind attack.

The force has the sum of sine shapes and operates only in the x direction, while the components in the y and z directions are zero.

The oscillatory characteristic of the response in all three directions x , y , z confirms that all these motions are coupled with each other.

There is a very good tracking of the desired trajectory at the frame of camera motion (see Fig. 6a) and Fig. 7a)) and at the frame of motor motion (see Fig. 6b) and Fig. 7b)).

The motor 1 enters the saturation at the start of simulation and stays there until to the end of the task. See Fig. 8a).

The second, third, and fourth motors do not enter saturation at all. The presented motor force load F_∇ with its components F_1 , F_2 , F_3 and F_4 , and their high oscillations caused by the disturbance force P_p are presented in Fig. 8b).

The oscillatory response in all three directions x , y , z exists at the end of the desired task.

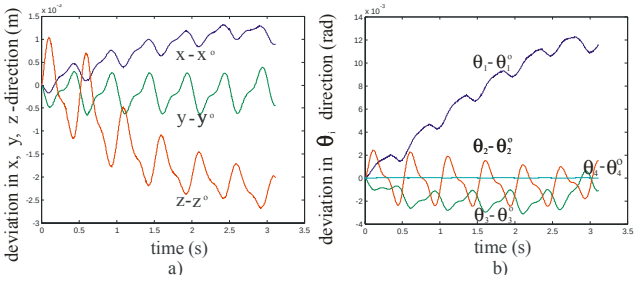

Figure 7. Real deviation from the reference frame values of a motion trajectory of a) camera carrier, b) the motor shaft.

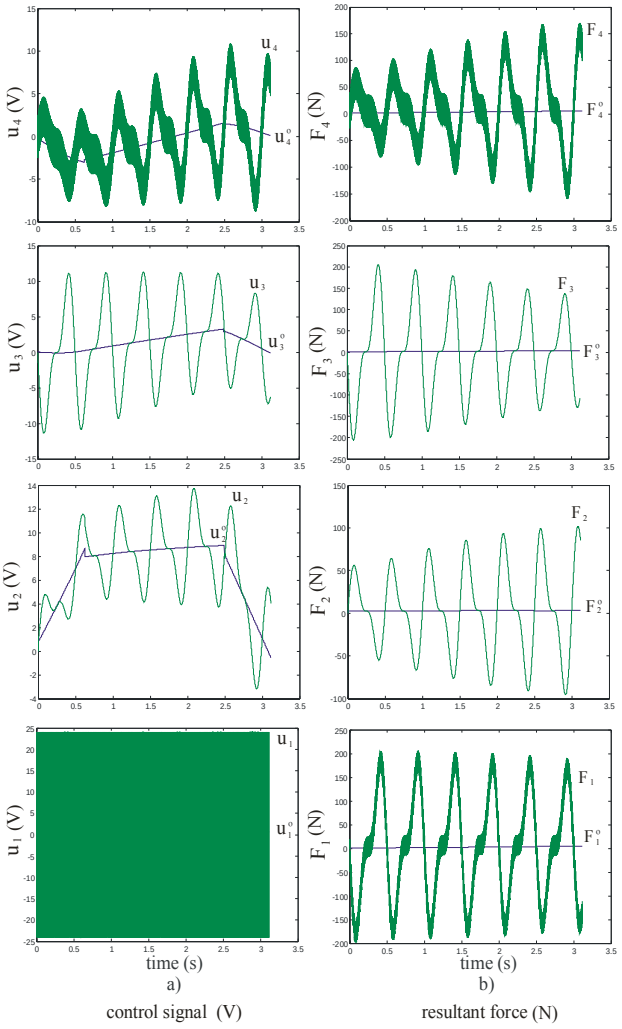

Figure 8. a) Rresultant forces acting on the shaft of each motor F_i , b) reference frame and real frame control signal u_i .

The presented results imply that the dynamics of the individual motor significantly depend of the selection of the CCPR structure and its parameters.

The example confirms the presence of coupling between all four motors, and between motors and camera carrier motion.

IV. CONCLUSION

High authentic form of CCPR mathematical model is defined for CCPR system. An adequate choice of generalized coordinates (in this paper, the internal coordinates), provides a mathematical model that illuminates the mapping of internal (forces in ropes) and external forces (acting on a camera carrier) on motion dynamics of each motor.

Software package ARRO are formed and used for analysis of CCPR from various aspects. The impact of changing any

parameter of the system (workspace dimensions, the mass of a camera carrier, change the size and dynamics of power disturbances, the choice of control law, the reference trajectory, and the presence of singularity avoidance system and a number of other characteristics) can be analyzed through these software packages.

The choice of motor characteristics, which are the important component of CPR, is especially emphasized. The simulation results present how a chosen motor type responds at mechanism characteristics change or at the presence of disorder such as not knowing some system characteristics or at the presence of disturbance forces. Motor type can significantly affect the response of the system or accuracy of tracking the desired trajectory.

Future research intend at implementing the elastic ropes (type of nonlinear dynamic elasticity as defined in [11]-[16]) in the mathematical model of the CPR-C. In this research several different models were developed and new models will be developing for different applications. All these models will be unified according to their similarities into one reconfigurable model, using the approached presented in [17] and [18]. The aim of this study is to define really the characteristics of CPR and all this for the purpose of modernization and wider application of the same.

ACKNOWLEDGMENT

This research was supported by the Ministry of Science and Technological Development of Serbia for financing the national research project "Ambientally intelligent service robots of anthropomorphic characteristics" TR-35003 and project "The dynamics of hybrid systems of complex structure", OI-174001. We are grateful to Prof. Dr. Katica R. (Stevanovic) Hedrih from Mathematical Institute, Belgrade for helpful consultations during the implementation of this paper.

REFERENCES

[1] C. Gosselin and J. Angeles, "The Optimum Kinematic Design of a Planar Three-Degree-of-Freedom Parallel Manipulator," Journal of Mechanisms, Transmissions, and Automation in Design, Vol. 110/35-41, March 1988.

[2] J. Fang and Z. Huang, "Kinematics of a three-degree-of-freedom in-parallel actuated manipulator mechanism," Mech. Mach. Theory, Vol. 32, No 7, pp. 789-796, 1997.

[3] P.H. Borgstrom, N. Peter. Borgstrom, M. J. Stealey, B. Jordan, G. Sukhatme, M. A. Batalin and W. J. Kaiser, "Discrete Trajectory Control Algorithms for NIMS3D, an Autonomous Underconstrained Three-Dimensional Cabled Robot," Proceedings of the 2007 IEEE/RSJ International Conference on Intelligent Robots and Systems, San Diego, CA, USA, Oct 29 - Nov 2, 2007.

[4] J. P. Merlet, MARIONET, "A Family of Modular Wire-Driven Parallel Robots," Advances in Robot Kinematics: Motion in Man and Machine, Part 1, pp. 53-61, 2010.

[5] M. Gouttefarde, J.-P. Merlet and D. Daney, "Determination of the wrench-closure workspace of 6-DOF parallel cable-driven mechanisms," Advances in Robot Kinematics, Part 5, 315-322, 2006.

[6] T. Bruckmann, L. Mikelsons, D. Schramm, M. Hiller, "Continuous workspace analysis for parallel cable-driven Stewart-Gough platforms," Special Issue: Sixth International Congress on Industrial Applied Mathematics (ICIAM07) and GAMM Annual Meeting, Zürich 2007, Volume 7, Issue 1, December 2007.

[7] A. Pott, "Forward Kinematics and Workspace Determination of a Wire Robot for Industrial Applications," Advances in Robot Kinematics: Analysis and Design, Part 7, 451-458, 2008.

[8] P. Miermeister, A. Pott, A. Verl, "Auto-Calibration Method for Overconstrained Cable-Driven Parallel Robots," ROBOTIK 2012 - 7th German Conference on Robotics, Munich, Germany, 2012.

[9] T. Higuchi, A. Ming, and J. Jiang-Yu "Application of multi-dimensional wire crane in construction," In 5th Int. Symp. on Robotics in Construction, pp. 661–668, Tokyo, June, 6-8, 1988.

[10] A. Rodic, M. Jovanovic, S. Popic, G. Mester, Scalable Experimental Platform for Research, Development and Testing of Networked Robotic Systems in Informationally Structured Environments, Symposium Series on Computational Intelligence SSCI, Paris,France, pp. 136-143, 2011.

[11] M. Filipović and M. Vukobratović, "Complement of source equation of elastic line," Journal of Intelligent & Robotic Systems, International Journal, Volume 52, No 2, pp. 233-261, June 2008.

[12] M. Filipović and M. Vukobratović, "Expansion of source equation of elastic line," Robotica, Cambridge University Press, pp. 1-13, 2008.

[13] M. Filipovic, Relation between Euler-Bernoulli Equation and Contemporary Knowledge in Robotics, Robotica, , Cambridge University Press. (2011) 1-13.

[14] K. (Stevanovic) Hedrih, "Dynamics of coupled systems," Nonlinear Analysis: Hybrid Systems, 2(2), pp. 310-334, 2008.

[15] K. (Stevanovic) Hedrih, Energy and Nonlinear Dynamics of Hybrid System, Chapter in Book Dynamical Systems and Methods, Edited by Albert Luo, Springer 1 (2012) 29-83.

[16] K. (Stevanovic) Hedrih, "Transversal vibrations of the axially moving sandwich belts," ARCH APPL MECH, 77(7), pp. 523-539, 2007.

[17] A. Djuric, R. Al Saidi, W. ElMaraghy, "Dynamics Solution of n-DOF Global Machinery Model", Robotics and Computer Integrated Manufacturing (CIM)" Journal, Vol. 28, Issue 5, pp. 621-630, 2012.

[18] A. M. Djuric, R. Al Saidi and W. H. ElMaraghy, (2010), "Global Kinematic Model Generation for n-DOF Reconfigurable Machinery Structure", 6th IEEE Conference on Automation Science and Engineering, CASE 2010, Toronto, Canada, August 21-24, 2010.